11th World Congress on Computational Mechanics (WCCM XI)
5th European Conference on Computational Mechanics (ECCM V)
6th European Conference on Computational Fluid Dynamics (ECFD VI)
E. Oñate, J. Oliver and A. Huerta (Eds)

# NUMERICAL SIMULATION OF WAVE LOADING ON STATIC OFFSHORE STRUCTURES

**Hrvoje Jasak[*,†], Inno Gatin[*] and Vuko Vukčević[*]**

[*] Faculty of Mechanical Engineering and Naval Architecture
University of Zagreb
Ivana Lučića 5, 10000 Zagreb, Croatia
e-mail: hrvoje.jasak@fsb.hr, ig185258@stud.fsb.hr, vuko.vukcevic@fsb.hr , web page: http://www.fsb.unizg.hr/

[†] Wikki Ltd
459 Southbank House, SE1 7SJ, London, United Kingdom
e-mail: h.jasak@wikki.co.uk, web page: http://wikki.gridcore.se/

**Key words:** CFD, Volume of Fluid, Two Phase Flows, Wave Loads, OpenFOAM.

**Abstract.** This paper presents numerical simulations with dominant free surface effects. Wave loads exerted on static offshore structures are calculated. Simulations are carried out using Finite Volume Method (FVM).
Mathematical model of two phase incompressible flow is based on Naiver-Stokes equations. Volume of Fluid (VOF) [4] method is used for interface capturing. Waves are generated using relaxation zones principle [3]. Pressure-velocity coupling is obtained by PIMPLE algorithm, a combination of SIMPLE and PISO algorithm. It allows calculations with higher Courant numbers, reducing required computational time. Simulations are calculated with OpenFOAM software package.
The method is validated with two test cases. In first simulation truncated vertical cylinder immersed in water is exposed to incoming waves. Forces on cylindrical column are calculated. Five cases of harmonic waves with different frequencies and wave heights are investigated. Data is compared with experimental results from [2]. The forces on the column in the direction of wave propagation show good agreement with experimentally measured forces. The second case describes freak wave initialization and simulation. Finally it is concluded that CFD simulations for given cases give acceptably accurate results.

## 1 INTRODUCTION

Designing offshore structures requires information about loads that might occur during their service. The safety margin depends on the reliability of information about loads.

Generally, smaller safety factors result in lesser production costs of structures, keeping in mind safety of crew members and material goods. In order to acquire more precise information about wave loads, Computational Fluid Dynamics (CFD) methods are getting more attention. The phenomenon of freak wave is especially dangerous for offshore structures, and calculation of freak wave loads is not an easy task using conventional methods. In this work, finite volume (FV) method is used in order to calculate wave loads on static structures in both regular and freak waves.

This paper is organized as follows. In section 2 governing equations for two phase flow are given and method for wave generation is presented. This includes Navier Stokes equations and Volume of Fluid (VOF) method. Next, in section **??** some details of numerical procedure are given. Section 4 presents considered test cases. Two test cases simulations are conducted in this paper. Finally, conclusion is given discussing the results of simulations.

## 2 MATHEMATICAL MODEL

In this section mathematical model of incompressible two-phase flow is presented. Continuity and momentum equations are shown, and equation on which Volume of Fluid method for interface capturing is based on [4]. Finally, wave modeling using relaxation zones is described [3].

### 2.1 Continuity and momentum equations

Numerical simulations are based on continuity equation (1) and momentum equation (2). For viscid Newtonian incompressible fluid the continuity equation can be expressed as:

$$\nabla \bullet \mathbf{u} = 0\,, \tag{1}$$

and the momentum equation is:

$$\frac{\partial \rho \mathbf{u}}{\partial t} + \nabla \bullet (\rho \mathbf{u}\mathbf{u}) = -\nabla p^* + \nabla \bullet (\mu \nabla \mathbf{u}) + \nabla \mathbf{u} \bullet \nabla \mu - \mathbf{f} \bullet \mathbf{x} \nabla \rho + \sigma \kappa \nabla \alpha\,. \tag{2}$$

Where $\mathbf{u}$ is the velocity field, $p^*$ is the dynamic pressure and $\alpha$ is the volume fraction. $\mathbf{f}$ presents gravitational force. According to [5], the last term models the surface tension effects. Furthermore, $\rho$ and $\mu$ present density and dynamic viscosity, respectively. For more details on the derivation of the above equation, reader is referred to [4].

### 2.2 Volume of Fluid equations

This method is based on $\alpha$ function [4] which is defined as:

$$\alpha = \frac{V_1}{V}\,. \tag{3}$$

Where $V_1$ is the volume of first phase (water) in the cell, and $V$ is the volume of the cell. Fluid properties need to be defined before the solution of momentum equation. Density and dynamic viscosity are obtained using the $\alpha$ indicator function:

$$\begin{aligned} \rho &= \alpha\rho_1 + (1-\alpha)\rho_2 \,, \\ \mu &= \alpha\mu_1 + (1-\alpha)\mu_2 \,. \end{aligned} \tag{4}$$

The transport equation for indicator function in VOF method is:

$$\frac{\partial \alpha}{\partial t} + \nabla\bullet(\mathbf{u}\alpha) + \nabla\bullet(\mathbf{u}^r\alpha(1-\alpha)) = 0 \,, \tag{5}$$

where $\alpha$ is the indicator function, defined as follows:

$$\alpha(\mathbf{x}) = \begin{cases} 1 \,, & \text{if } \mathbf{x} \in \Omega_1 \,, \\ 0 < \alpha < 1 \,, & \text{if } \mathbf{x} \textit{ in the transitional area} \,, \\ 0 \,, & \text{if } \mathbf{x} \in \Omega_2 \,. \end{cases} \tag{6}$$

$\Omega_1$ is the part of the domain that is occupied by the first phase (water), while $\Omega_2$ is the part of the domain containing the second phase (air). Cells that contain the free surface have the value of $\alpha$ between 0 and 1. Third term on the left of the equation (5) is the $\alpha$ compression term [8].

### 2.3 Wave modelling using relaxation zones

Wave modeling is conducted with coupling of potential flow wave theories and CFD solutions. Relaxation zones are used [3] to smooth out the transition between wave theory and CFD calculations. Coupling is done inside the relaxation zone, while outside only CFD solution is used. One of the biggest problems with wave modeling is damping the waves at the end of the wave tank in order to prevent the reflected waves to pollute the results. This method uses outlet relaxation zone, in which coupling is also made between CFD solution and calm free surface solution, which includes constant velocity on the whole depth of the relaxation zone.

The variables are coupled using weight function $f_R$ as follows:

$$\phi = f_R\phi_{target} + (1-f_R)\phi_{computed} \,. \tag{7}$$

where $\phi_{target}$ is the value of the variable obtained from the wave theory or the conditions for the outlet zone, while $\phi_{computed}$ is the value for the same variable calculated by CFD algorithm.

## 3 NUMERICAL PROCEDURE

PIMPLE algorithm is used for pressure-velocity coupling. PIMPLE is an algorithm that uses a few PISO correctors per each SIMPLE corrector. As well as momentum and pressure equations, VOF transport equation (5) is also treated implicitly. Implicit solving enables higher Courant numbers. In this paper two SIMPLE correctors and four PISO correctors are used per each time step. Second order accuracy in space is achieved. For temporal discretization Euler implicit scheme is used, and for convective terms van Leer scheme is mostly used [9].

## 4 TEST CASES

Two types of simulations are carried out using OpenFOAM's navalHydro pack. First simulation is used to validate accuracy of the numerical simulation for regular waves. Wave loads on vertical cylinder are calculated and results are compared with experimental data from [2]. Second case shows the possibility of freak waves simulation using OpenFOAM.

### 4.1 Harmonic wave loads on vertical cylinder

In this chapter results of CFD simulations of wave loads on vertical cylinder are presented for five different incoming waves. Results are compared to experimental results presented in [2].

The experimental measurements are carried out in a tank 36.5 m long, 2.4 m wide and 1.5 m deep. Circular cylinder is vertically immersed in water to the depth of 27 cm, it does not reach the bottom of the tank. Cylinder diameter is 89 mm, and it is placed at 13.7 m from the wave maker. At the opposite end of the tank from the wave marker, a sloping beach is placed for wave absorption. There is enough room between the cylinder and the beach for the force measurements to be carried out before the reflected waves reach the cylinder, polluting the results. In [2] maximum measured forces in the longitudinal direction are given. Maximum of forces are determined over ten wave periods for each wave. The measurements are carried out for wave frequencies of 1.43, 1.1, 1.0, 0.9 and 0.7 Hz. For each frequency ten wave slopes ranging from 0.06 to 0.24 are used, where $k\eta$ is the wave slope, $k$ is wave number and $\eta$ wave amplitude according to Airy wave theory. Five waves are selected for numerical calculation. Wave parameters used in simulations are presented in Tab. 1.

The domain is reduced comparing to experimental setup to save computational time. Length of the domain is shortened to three wave lengths. In the simulation the long tank is not needed since waves are absorbed completely in outlet relaxation zone. Length of the inlet relaxation zone is set half of the wave length, while the outlet relaxation zone is one wave length long. Smaller outlet relaxation zones proved to be reflective.
Fig. 1 shows the finite volume mesh in horizontal plane near the cylinder. Mesh used for calculations has 1 728 490 cells. Maximum aspect ratio of cells is 1:47. Linear grading

Table 1: Incident wave parameters.

| Index N | Frequency $f$, hz | Wave slope $k\eta_a$, rad | Wave number $k$, rad/m | Wave height $h$, m | Wave length $\lambda$, m | Period $T$, s |
|---|---|---|---|---|---|---|
| 1 | 0.70 | 0.06 | 1.97 | 0.060 | 3.19 | 1.43 |
| 2 | 0.70 | 0.12 | 1.97 | 0.120 | 3.19 | 1.43 |
| 3 | 0.90 | 0.20 | 3.26 | 0.123 | 1.93 | 1.11 |
| 4 | 1.10 | 0.12 | 4.87 | 0.050 | 1.30 | 0.90 |
| 5 | 1.43 | 0.20 | 8.83 | 0.049 | 0.76 | 0.70 |

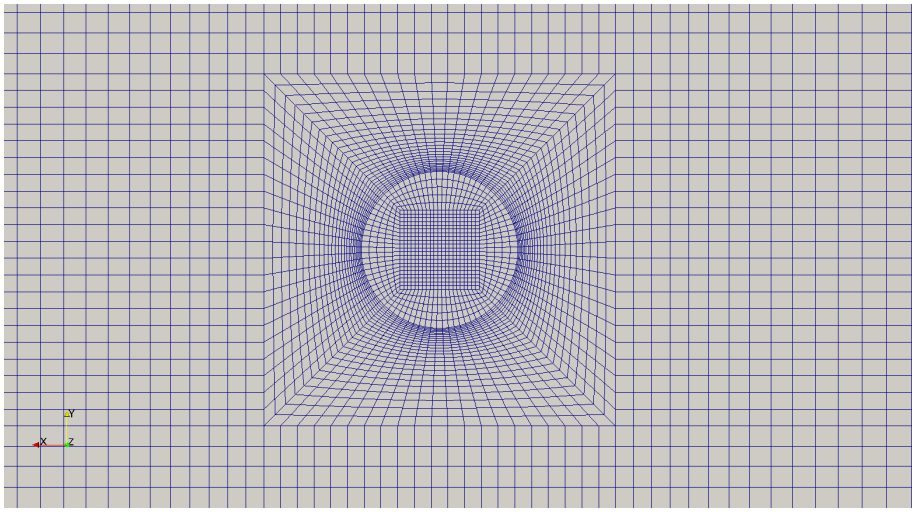

Figure 1: Mesh geometry near the cylinder.

is used to refine the mesh around the cylinder, and as a result cells near the cylinder are 140 times smaller that those on the edge of the domain.

Loading forces in longitudinal direction are obtained for each wave type from Tab. 1. Fig. 2 shows a force signal for the simulation of wave index number 3 from Tab. 1. Tab. 2 presents the comparison of the results obtained by numerical calculation and experimental results for each wave from Tab. 1. For waves 1,2 and 3 the errors are acceptable. For higher frequencies the errors are larger. The accuracy of the calculation depends on the vertical mesh refinement, i.e. on the number of cells per wave height, and on wave frequency. Results also show some dependency on Courant number. For waves 4 and 5 finer mesh is used. It can be seen in Tab. 2 that the error for wave 5 is significantly smaller. It should be noted that finer mesh used for waves 4 and 5 is still relatively coarse mesh considering domain size, and it is believed that further refinement would improve the result.

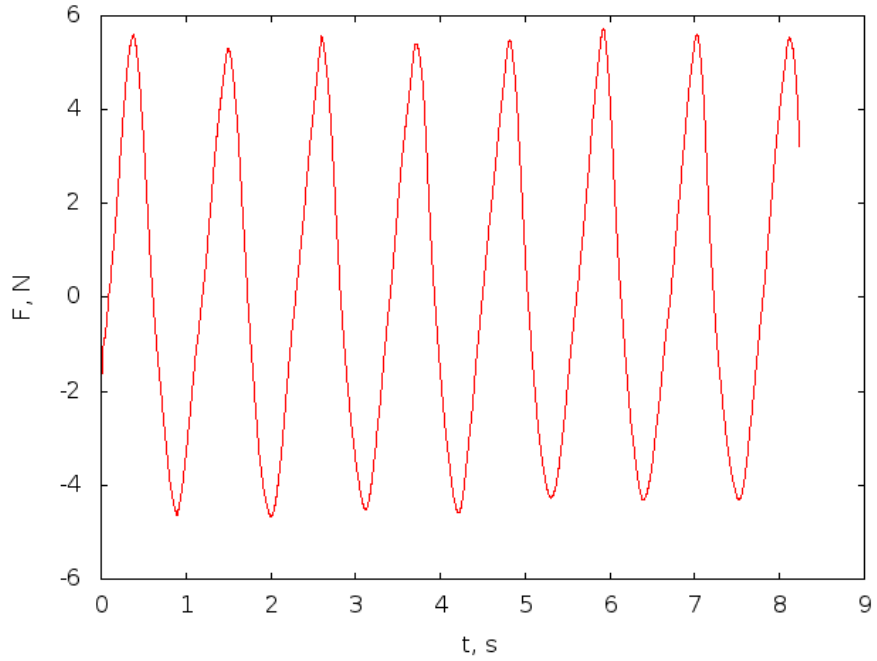


Figure 2: Force signal for wave index 3 (Tab. 1).

Table 2: Comparison of CFD and experimental results.

| Wave index N | CFD results $F_x$, N | Experimental results $F_x$, N | Relative error $Err$, % | Number of cells | Courant number $Co$ | $\alpha$Courant number $\alpha Co$ |
|---|---|---|---|---|---|---|
| 1 | 1.778 | 1.80 | 1.22 | 1 728 490 | 6.0 | 3.00 |
| 2 | 4.790 | 5.00 | 4.20 | 1 728 490 | 6.0 | 3.00 |
| 3 | 5.573 | 5.70 | 2.23 | 1 728 490 | 2.0 | 1.50 |
| 4 | 2.390 | 2.80 | 14.64 | 1 728 490 | 1.5 | 0.75 |
| 4 | 2.361 | 2.80 | 15.68 | 2 805 810 | 1.5 | 0.75 |
| 5 | 2.650 | 3.08 | 13.96 | 1 728 490 | 2.0 | 1.50 |
| 5 | 2.854 | 3.08 | 7.34 | 2 629 410 | 2.0 | 1.50 |

### 4.2 Freak wave simulation

Freak wave, also known as rouge wave, is a phenomenon that is not fully understood [6]. Moreover, there is no generally accepted definition of a freak wave. According to the definition that is most widely accepted, a freak wave is a wave which height exceeds the significant wave height of the current sea state by two times [6]. Freak wave has a low probability of occurrence, but it poses a great threat to offshore structures and ships which is why new methods of calculating freak wave loads are getting more attention.

Method of harmonic wave focusing is used to generate the freak weave. Harmonic waves used for focusing are components of Pierson-Moskowitz sea spectrum. This is done in order to obtain a more realistic freak wave, since sea spectrum describes realistic sea states. Free surface elevation is determined by superimposing individual harmonics. For this simulation, 30 wave components are used, guided by recommendation in [7]. Phase shifts of the wave components are usually selected from a uniformly distributed random numbers. This ensures that the reproduced sea state is statistically equal to the sea state on which the wave energy spectrum is determined. However, to initialize a freak wave, phase angles must be set in the way that will ensure positive superposition of the wave components in order to achieve extreme wave height at desired time and position. Thus phase shifts are found by optimization procedure. Freak wave obtained by linear superposition of wave components is 0.255 m high, which is 2.12 times higher then selected significant wave height of 0.12 m. This qualifies this wave as a freak wave according to the widely used definition [6].
Fig. 3 depicts freak wave profile in the simulation shortly before focusing time of 2.66 s. Blue color shows the part of the domain which contains water ($\alpha = 1$), red color shows the air in the domain ($\alpha = 0$). Green color shows the transitional area between air and water, i.e. values of $\alpha$ are between 0 and 1. Thick horizontal white line in Fig. 3 is positioned at calm free surface level. Thinner white horizontal lines show positive and negative significant amplitudes, i.e. distance between them is the significant wave height. Black horizontal lines are positioned at the bottom and top of the freak wave. Height difference is obvious, and it agrees well with the calculated height. White vertical line shows the position of the cylinder centerline.
Fig. 4 shows a frame shot of simulation at the same moment of time as in Fig. 3. Further propagation of the freak wave caused further steepening of the front wave slope. Fig. 5 shows simulation frame shot in the moment of impact against the vertical cylinder. It can be observed that that the wave slope was close to vertical at moment of impact. That is in accordance with often encountered description of freak wave as a wall of water.

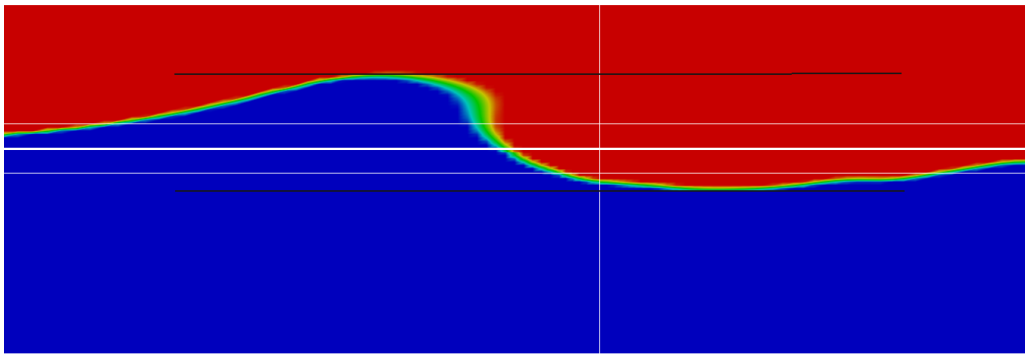

Figure 3: Freak wave profile during simulation.

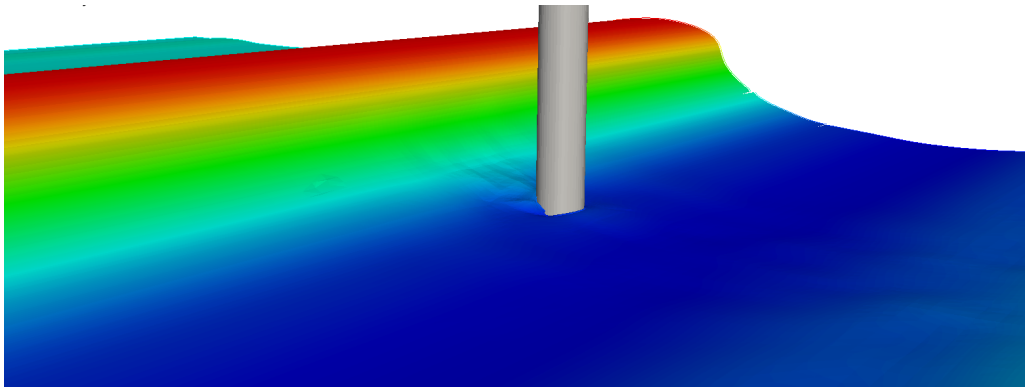

Figure 4: Frame shot at the moment before wave impact.

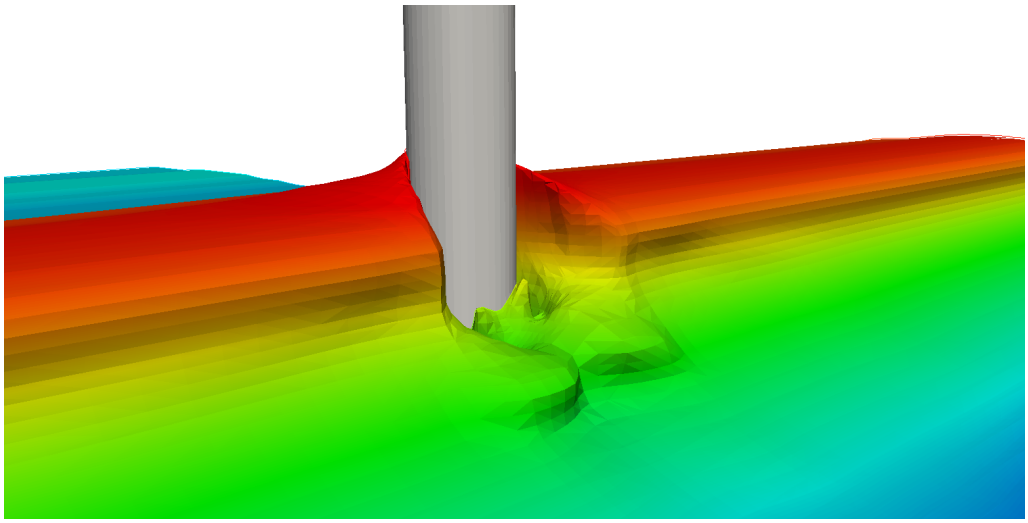

Figure 5: Frame shot at the moment of wave impact.

## 5 CONCLUSION

Numerical simulations of two cases are carried out which have practical application in modern offshore industry. For domain discretization Finite Volume Method is used, while VOF method is used for interface capturing.

Presented test cases show good results. First case shows very good agreement with experimental results. Second case presents the possibility of evaluating loads on offshore structures and ships exerted by the freak wave, which is hardly achievable by other methods. The results show that numerical simulations in OpenFOAM can indeed be used in the process of designing offshore structures in general. Considerable savings could be made due to resulting smaller safety margins of structures and smaller price of obtaining results in comparison with experimental methods.

## REFERENCES

[1] Gómez-Gesteira, M. *SPHERIC SPH benchmark test cases: Test 1-Force exerted by a schematic 3D dam break on a square cylinder*. `http://cfd.me.umist.ac.uk/sph/TestCases/SPH_Test1.html`, 2006.

[2] Boo, S.Y. *Measurments of higher harmonic wave forces on a vertical truncated circular cylinder*, Ocean Engineering, Vol **33**, 219 – 233, 2006.

[3] Jacobsen, N. G., Fuhrman, D. R., Fredsøe, J. *A Wave Generation Toolbox for the Open Source CFD library: OpenFoam*, International Journal for Numerical Methods in Fluids, Vol **9**, 1078 – 1088, 2012.

[4] Ubbink, O. *Numerical prediction of two fluid systems with sharp interfaces*, Imperial College of Science, Technology & Medicine, London, 1997.

[5] BrackBill, J. U., Kothe, D. B., Zemnach, C. *A Continuum Method for Modelling Surface Tension* Journal of Computational Physics, Vol. **100**, 335–354, 1992.

[6] Kharif, C., Pelinovsky, E. *Physical mechanisms of the rogue wave phenomenon*, European Journal of Mechanics - B/Fluids, 2003, Vol. **22**, 603-634.

[7] Zhao, X. *Numerical simulation of extreme wave generation using VOF method*, Jurnal of hydrodynamics, 2010, Vol. **22**, 466-477.

[8] Rusche, H. *Computational Fluid Dynamics of Dispersed Two Phase Flows at High Phase Fractions*, Imperial College of Science, Technology & Medicine, London, 2002.

[9] van Leer, B. *Towards the Ultimate Conservative Difference Scheme. IV. A New Approach to Numerical Convection* Journal of Computational Physics, Vol. **23**, 276–299, 1977.